Published in final edited form as:
Virology. 2010 March 15; 398(2): 201–207. doi:10.1016/j.virol.2009.11.046.

Accelerated Evolution of SIV *env* within the Cerebral Compartment in the Setting of Morphine-dependent Rapid Disease Progression

Vanessa Rivera-Amill[a,*], **Richard J. Noel Jr.**[b], **Yashira García**[a], **Ivelisse Rivera**[a], **Marcus Iszard**[d], **Shilpa Buch**[c], and **Anil Kumar**[d]

[a]Department of Microbiology, Ponce School of Medicine, Ponce, PR 00732

[b]Department of Biochemistry, Ponce School of Medicine, Ponce, PR 00732

[c]Department of Pharmacology, University of Nebraska Medical Center, Omaha, NE, USA

[d]Department of Pharmacology, School of Pharmacy, University of Missouri, Kansas City, KS, 64108, USA

Abstract

Human immunodeficiency virus-1 (HIV-1) and simian immunodeficiency virus (SIV) have been shown to compartmentalize within various tissues, including the brain. However, the evolution of viral quasispecies in the setting of drug abuse has not been characterized. The goal of this study was to examine viral evolution in the cerebral compartment of morphine-dependent and control macaques to determine its role in rapid disease progression. To address this issue, we analyzed the envelope (*env*) gene from proviral DNA in our SIV/SHIV macaque model of morphine-dependence and AIDS. Analyses of proviral DNA revealed a direct correlation between total genetic changes and survival time. However, the rate of evolution during disease progression was higher in morphine-dependent and rapid-progressor macaques than was the rate of evolution in the control animals. This study provides additional insight into SIV envelope variation in the CNS of morphine-dependent macaques and genotypes that may have evolved in the brain and contributed to disease progression.

Introduction

Drug abuse and dependence are widespread in the general population in many parts of the world and intravenous drug use is thought to play a major role in spread of the human immunodeficiency virus-1 (HIV-1) through engagement in a number of high-risk behaviors, including sharing needles and sexual contact.

The occurrence of HIV-1 infection in the context of drug abuse raises important questions about the potential interactions between the two phenomena. This is particularly significant considering that a large proportion of drug abusers are also HIV-1-infected individuals (2002;2003;Alcabes & Friedland, 1995;Chu & Levy, 2005;Cohn, 2002;Des, 1999). As of 2006, the Centers for Disease Control had estimated that there were 540,436 deaths in the

*To whom correspondence and reprint request should be addressed at Department of Microbiology, Ponce School of Medicine, Ponce PR 00732-7004, Fax (787)841-5150; vrivera@psm.edu.

United States of persons with AIDS, of which approximately 28% of the total were injection drug users (IDUs) (Centers for Disease Control and Prevention, 2008). The most widely abused drugs in the United States include heroin, cocaine and methamphetamine. However, the majority of IDUs report using multiple drugs at different times, thus it is difficult to directly link a specific drug to the observed clinical health parameters. Although numerous studies have documented that HIV-1-infected IDU experience substantial pre-AIDS morbidity, the natural history and progression of HIV-1 infection among IDU remains uncertain. Regardless, both *in vitro* and *in vivo* studies have demonstrated a correlation between drugs of abuse and increased viral replication (Chuang, Killam, Jr. et al., 1993;Nyland, Specter et al., 1998;Guo, Li et al., 2002;Suzuki, Chuang et al., 2002;Kumar, Orsoni et al., 2006).

HIV-1 and simian immunodeficiency virus (SIV) infections lead to neurological complications, and drug abuse is thought to adversely affect this occurrence in humans. Although antiretroviral therapy has proven effective in reducing the viral load in the central nervous system (CNS) with a resulting improvement in neurological function, viral reservoirs persist in the brain (reviewed in: (Dunfee, Thomas et al., 2006). Understanding viral evolution in the brain will help determine the viral factors that contribute to neurological disease.

The SIV/macaque model is particularly valuable for evaluating information that is usually impossible to obtain from human studies, such as the genotypic and phenotypic properties of the infecting virus, knowledge of the exact time of virus exposure, assessment of disease progression, and the characteristics of viral variants in the infected host. Whereas compartmentalization has been well demonstrated for both HIV-1 and SIV, few studies have characterized the impact of drugs of abuse on the degree of SIV *env* evolution and the role such viral dynamics may play in the rate of disease progression. Our model of SIV/SHIV infection and drug abuse offers a unique opportunity to address these important questions. We have previously shown a negative correlation between evolution of viral accessory genes in plasma and cerebrospinal fluid (CSF) and opiate-mediated disease progression (Noel, Jr. & Kumar, 2007;Noel, Jr., Marrero-Otero et al., 2006;Tirado & Kumar, 2006;Noel, Jr. & Kumar, 2006). In addition, we have also shown a positive correlation between the evolution of virus envelope and opiate-mediated disease progression (Rivera-Amill, Noel, Jr. et al., 2007). In this study we wanted to investigate the pathogenic and biologic consequences of SIV envelope sequence variation within the brain in morphine-dependent and control macaques infected with SIV/SHIV. In this report, the sequences of SIV/17E-Fr envelope gene recovered from the brain of morphine-dependent macaques are described. The results indicate that the highest levels of nucleotide substitution in sequences isolated from the brain were observed in animals that survived for longer periods, regardless of whether they were morphine dependent or not. Although the total diversity was most closely related to duration of infection, the rate of evolution was fastest for the morphine-dependent rapid disease progressors, who showed a rapid accumulation of changes early during infection.

Results

Clinical disease parameters of the six morphine-dependent and three control macaques used in this study are shown in Table 1. Half of the morphine-dependent macaques developed rapid disease progression (1/04L, 1/42N and 1/28Q). These macaques maintained high viral loads both in plasma and CSF, and low $CD4^+$ T cell counts. In contrast, morphine-dependent normal progressors (1/56L, 1/02N and 1/52N) and control macaques (2/02P, 2/AC42 and 2/31P) exhibited lower viral loads, and higher $CD4^+$ T cell counts. Two normal progressors and two control macaques exhibited CSF viral loads below the level of detection (Table 1). In order to determine whether viral DNA persisted in these macaques, genomic DNA from brain tissue was isolated and used for Real Time PCR to quantitate SIV/17E-Fr in the brain. Using *env* specific primers and probe, we demonstrated the presence of SIV/17E-Fr in the brain tissue

from morphine-dependent and control macaques despite significant down-regulation of viral RNA in the CSF (Table 1). Viral DNA in the brains of morphine-dependent and control animals was detected at similar levels and there were no statistically significant differences among the groups. These results, are in agreement with a previous study of SIV encephalitis by Clements et al., where they revealed that despite significantly lower levels of viral RNA in the brain after the acute phase, the DNA levels remained constant (Clements, Babas et al., 2002). Therefore, even though viral load in the CSF of two morphine-dependent normal progressors and two control macaques at the time of death were below the level of detection, virus-infected cells were not cleared. We were able to detect SIV RNA in brain tissue albeit at low levels and there were no significant differences between morphine dependent and control macaques (Table 1). Pathological changes in the brains of morphine-dependent macaques with neurological symptoms were characterized by accumulation of macrophages in the perivascular region (Figure 1A), focal histiocytic nodules (Figure 1B) and multi-nucleated giant cells (Figure 1C), characteristic of lentiviral encephalitis. Next we analyzed the SIV/17E-Fr *env* gene from the DNA isolated from morphine-dependent and control macaques in order to determine whether there are remarkable differences in the viruses that had established in the brain. Based on our previous study (Rivera-Amill, Noel, Jr., Orsini, Tirado, Garcia, Buch, & Kumar, 2007), we focused this analysis on SIV *env* V3-V5. In the present study we analyzed the diversity, divergence, synonymous and non-synonymous substitutions, as well as amino acid mutations in key functional regions in order to characterize SIV *env* evolution within the CNS.

Phylogenetic analysis of *env* clones from brain tissue

Phylogenetic analyses using SIV *env* V3V5 sequences derived from genomic brain DNA were carried out to determine the relatedness of variants between morphine-dependent and control macaques. Five to ten clones from each macaque were sequenced, aligned and subjected to phylogenetic analysis using the distance-based (neighbor-joining) method. The SIV/17E-Fr *env* sequence was used as the root for the trees. Bootstrap resampling using 500 replicate trees was carried out to estimate the robustness of the observed groupings. Phylogenetic trees of the morphine-dependent and control macaque brain-derived clones revealed clustering of the majority of the sequences derived from rapid progressors and a mixed distribution for some of the sequences derived from normal progressors and control macaques (Figure 2). Greater branch lengths were observed in the phylogenetic reconstruction for morphine-dependent normal progressors and control macaques, whereas rapid progressors exhibited less clonal diversity. When taking into consideration the average survival time for each group (rapid progressors 19 weeks; normal progressors 124 weeks; control macaques 90 weeks), we find that the rapid progressors exhibited a higher rate of mutations as compared to the other groups and that the sequences isolated from this group appear ancestral to the sequences isolated from the other macaques.

Diversity and divergence in brain-derived viral populations

We next calculated the nucleotide diversity of env V3-V5 region from brain samples focusing on group average calculations using MEGA 3.1. There was no significant difference in overall diversity between the clones derived from rapid- and normal- morphine-dependent and control macaques. However, analysis of the divergence from the inoculum revealed a statistically significant difference between rapid progressors and control macaques, whereas no difference was detected when comparing normal progressors to either rapid progressors or control macaques (Figure 3). When focusing exclusively on the V4 loop subregion, however, there was a significant reduction in the divergence of the brain-derived sequences from rapid progressors as compared to both normal progressors and control macaques (Figure 4). The patterns of diversity of the clones did not differ when comparing the groups. Previously, we found a direct correlation between SIV *env* V4 evolution and rapid disease progression when analyzing *env* sequences CSF by 12 weeks post-infection (wpi) (Rivera-Amill, Noel, Jr.,

Orsini, Tirado, Garcia, Buch, & Kumar, 2007). By 18 wpi, the morphine-dependent macaques still exhibited greater diversity and divergence as compared to control macaques. However, the morphine-dependent normal progressors had started to exhibit an increase in divergence as compared to rapid progressors. When analyzing sequences from the morphine-dependent normal progressors at a later time point, 32 wpi, we found that both the diversity and divergence (1.73% and 1.30%, respectively) of the clones from morphine-dependent normal progressors were higher than at 18 wpi although this difference was not significant.

Synonymous and non-synonymous nucleotide substitution rates

We analyzed the relative rates of synonymous (dS) and non-synonymous (dN) nucleotide substitutions in *env* V3V5 to assess selection pressures between the groups. For all of the samples analyzed, the dN rates were lower than the dS rates suggesting that positive selection did not play a role as the force driving the evolution of the *env* gene and that there was a bias toward silent substitutions in this region of *env* (Figure 5). Morphine-dependent rapid progressors exhibited significantly fewer silent and non-silent substitutions when compared to both morphine-dependent normal progressors and control macaques, supporting the idea that positive selection forces were not distinct among rapid progressors. In contrast, there was no significant difference between the normal progressors and control macaques.

Genotypic analysis of *env* regions

SIV *env* V3V5 brain sequences were compared for their differences in the number of positively charged amino acid residues in the V3, V4, V5 loops and changes within the GGDPE motif of the CD4 binding region. The net charge of each region was calculated by subtracting the number of negatively charged amino acids from the number of positively charged amino acids. Analysis of the amino acid changes and net charge within V3 and V5 loops of all clones isolated from morphine-dependent and control macaques revealed no significant differences in the frequency of amino acid mutations and overall changes in the net charge for any of the groups (data not shown). Within the V4 loop (Figure 6), morphine-dependent macaques exhibited a slight decrease in both the frequency of amino acid mutations (1.29) and the overall charge (2.85) as compared to control macaques that exhibited higher frequency of amino acid mutations (2.24) an increase in the overall charge within this region (3.19). However, this difference was only significant when comparing morphine-dependent rapid progressors and control macaques.

As shown in Figure 7, the mean frequency of amino acid mutations within the GGDPE motif was lower for the rapidly progressing morphine-dependent macaques as compared to normal progressors and controls. However, this difference was significant only when comparing rapid progressors to control macaques. Analysis of the changes of the net charge within this motif revealed that the rapid progressors maintained a higher overall negative charge as compared to normal progressors and control macaques for which most of the clones had a D385G change within this region. Analysis of previously reported sequences from CSF revealed that the rapid progressors demonstrated a similar frequency of amino acid mutations (0.326) as was seen in brain samples (Rivera-Amill, Noel, Jr., Orsini, Tirado, Garcia, Buch, & Kumar, 2007). However, the normal progressors and controls exhibited a lower frequency of amino acid mutations by 18 wpi (0.704 and 0.067, respectively) than was observed in the brain samples. Interestingly, in plasma-derived sequences, changes within this motif were frequently detected in rapid disease progressors at a high frequency, whereas in morphine-dependent normal progressors and control macaques very few clones exhibited changes in this region. In contrast to the normal progressors and control macaques, the rapid disease progressors were unable to mount a neutralizing humoral response (Kumar, Orsoni, Norman, Verma, Tirado, Giavedoni, Staprans, Miller, Buch, & Kumar, 2006). Collectively, these data suggest that changes within this region occurred independently of selective pressures from the immune system.

A D385N change has been reported from SIVmac239 infected animals that progressed rapidly to simian AIDS (SAIDS) and this change, in addition to G383Rwhich is frequently found together with D385N, resulted in a greater decrease in CD4 binding (Ryzhova, Whitbeck et al., 2002). None of the SIV/17E-Fr clones reported here exhibited the G383R change. Conversely, even though these changes were found to be associated with enhancement of CD4-independent cell to cell fusion, it has been reported that analysis of individual changes in SIVmac239 D385N or D385G result in decreased viral infectivity (Otto, Puffer et al., 2003), suggesting that additional changes must also be selected for efficient viral replication and spread.

Discussion

In this study, the morphine-dependence SIV/SHIV macaque model was used to investigate SIV *env* sequence variation in the brain, because macaques are common models for Neuro-AIDS. The use of a cocktail of molecularly cloned viruses allowed for the close monitoring of viral genetic variation. The changes within SIV *env* V3V5 region in brain were examined in six morphine-dependent and three control macaques that were all infected with SIV/17E-Fr, $SHIV_{KU-1B}$ and $SHIV_{89.6}$P to understand the evolution of viral genes and their contribution to disease progression and neurological disease.

A number of studies have focused on *in vivo* SIV *env* evolution in both rapid and slow disease progressors. Despite the fact that rapid progressors exhibit an apparent lack of immune pressure due to the absence or transience of humoral and cellular immune responses and they maintain high viral loads throughout infection, SIV *env* undergoes unique changes within this group. Although the details of the animal model used were different as compared to the present study, in a report by Chen et al., analysis of SIVmac239 *env* evolution in the central nervous system (CNS) revealed that long-term progressing macaques demonstrated a greater degree of compartmentalization and higher synonymous and non-synonymous substitution rates as compared to the rapidly progressing macaques (Chen, Westmoreland et al., 2006). However, in their study they were unable to analyze sequential plasma or CSF samples to determine how the changes were accumulating. In contrast, in a study by Dehghani et al., the investigators reported that substitutions within the V3 loop and GGDPE motif of SIVsmE543-3 characteristic of all rapid progressors studied were not observed in slow progressors by 52 wpi (Dehghani, Puffer et al., 2003). At later times post-infection they determined that in rapid progressors, virus variants appear to be adapted to replicate *in vivo* but are at a disadvantage to replicate in tissue culture as compared to the parent strain (Kuwata, Dehghani et al., 2006). However, samples from the slow progressors taken near the time of death were not reported in these studies. Thus it remains unclear as to whether the changes in *env* could have accumulated at a later time point in slow progressors. Other studies have also focused on SIV *env* evolution but have not distinguished between animals with different rates of disease progression (Kinsey, Anderson et al., 1996). It should be emphasized that none of the studies reported drug abuse as a confounding factor.

In our earlier analysis of SIV *env* evolution in plasma and CSF, we found direct correlation of SIV *env* V4 region and disease progression at 12 wpi, i.e. the morphine-dependent rapid progressors exhibited more diversity and divergence of the clones than morphine-dependent normal progressors and control macaques (Rivera-Amill, Noel, Jr., Orsini, Tirado, Garcia, Buch, & Kumar, 2007). By 18 wpi, the normal progressors exhibited a higher trend of divergence as compared to the rapid progressors although this difference was not significant. Both morphine-dependent sub-groups exhibited increased diversity and divergence as compared to control macaques. Analysis of viral diversity and divergence within the morphine-dependent normal progressors at a later time point, 32 wpi, revealed that the normal progressors exhibited a diversity of 1.73% and a divergence of 1.30% slightly higher, although not at a

level of statistical significance, than the last time point recorded for the rapid progressors (unpublished data). We were unable to amplify SIV *env* from control macaques at 32 wpi. In this study, we analyzed SIV proviral *env* evolution in brain tissue. When comparing the rapid progressor brain sequences to plasma and CSF sequences from the time of death, like before, we found a significant difference between plasma and brain. No significant differences were detected in the diversity and divergence when comparing brain and CSF isolated sequences, indicating that the actively replicating viral forms detected in the CSF of rapid disease progressors were from the viral forms established in the brain. However, when including in the analysis samples from morphine-dependent normal progressors and control macaques, we found an inverse correlation between sequence diversity and disease progression, i.e. the rapid progressors exhibited less diversity and divergence in brain isolated sequences as compared to morphine-dependent normal progressors and control macaques. Although we were unable to amplify SIV from plasma and CSF samples from morphine-dependent and control macaques near the time of death (viral loads were below the level of detection), as explained above, the trend was that the macaques that survived longer demonstrated an increase in both diversity and divergence as compared to the rapidly progressing macaques. Thus, sequence changes were accumulating at a faster rate in morphine-dependent rapid progressors as compared to morphine-dependent normal progressors and control macaques. These results suggest that the genetic variation observed in the brain sequences from morphine-dependent normal progressors and control macaques was a consequence of the difference in length of survival rather than a result of a higher rate of accumulation of mutations and perhaps morphine does not alter selection but only quickens evolution initially as seen in rapid progressors. Furthermore, our immunohistochemical findings also suggest evidence of increased dissemination of virus in various peripheral tissues (data not shown) with concomitant neuropathological changes in the morphine-dependent animals.

Current work is in progress in our laboratory to address whether these observations correlate with the analysis of SIV *env* evolution in other compartments as well as the functional characterization of these changes. Work is also underway to determine whether other genotypes are also present in the brain. Further studies are needed to define the role of *env* and other viral genes in the development of rapid disease progression and neuroAIDS in the setting of drug abuse.

Methods

Animal Model

Establishment of morphine addiction has been previously described (Kumar, Torres et al., 2004). Briefly, morphine dependence was established by injecting increasing doses of morphine (1 to 5 mg/kg of body weight over a two-week period) by the intramuscular route at 8-h intervals. The animals were maintained at three daily doses of morphine (5 mg/kg) for an additional 18 weeks. All macaques were infected by the intravenous route with a 2-ml inoculum containing 10^4 50% tissue culture infective doses each of simian-human immunodeficiency virus $SHIV_{KU-1B}$ (Singh, McCormick et al., 2002), SHIV $_{89.6}$P (Reimann, Li et al., 1996a;Reimann, Li et al., 1996b) and SIV/17E-Fr (Flaherty, Hauer et al., 1997). All animals were perfused before euthanasia to remove PBMCs. The experimental protocol was approved by the Institutional Animal Care and Use Committee, and the research was conducted in accordance with the Guide for the Care and Use of Laboratory Animals.

Viral RNA in plasma and CSF

Cell-free viral loads in plasma and CSF were determined in duplicate by real-time reverse transcription-PCR (RT-PCR) (Amara, Villinger et al., 2001). The viral RNA copy number in macaque samples were determined by comparison with an external standard curve consisting

of in vitro transcripts from the SIVmac239 genome. This assay has a sensitivity of 80 copies/ml of plasma or CSF.

Immunohistochemical staining

Immunohistochemical analyses were performed on paraffin-embedded tissues. Paraffin embedded tissue sections were deparaffinized in xylene for 30 minutes and rehydrated in graded series of alcohol. Following washes in PBS and blocking in donkey serum for 30 minutes, sections were incubated in primary murine monoclonal antibodies to p27, the Gag protein of SIV (Advanced Biotechnologies Inc, Maryland, USA); followed by treatment with biotinylated goat anti-mouse IgG (DAKO, Carpenteria, California, USA), peroxidase-conjugated streptavidin (DAKO), and NovaRed substrate (Vector Laboratories, Burlingame, California, USA), which yields a reddish reaction product (Hicks, Potula et al., 2002). Cells positive for p27 were counted using a 40× objective. For each sample, 70 different fields were evaluated and the number of positive cells was calculated for the total area of the fields.

Tissue collection and processing

Tissue specimens were obtained from our archived collection of rhesus macaque tissues at Ponce School of Medicine. DNA from tissues was isolated using the QIAmp DNA Blood and Tissue Kit (Qiagen, Inc., Valencia, CA) according to the manufacture's recommendations.

Viral DNA and RNA in brain tissue

To quantitate viral DNA and RNA in brain tissue, genomic DNA and total RNA were isolated from duplicate samples of frozen tissue using DNeasy Tissue Kit and RNeasy kit (Qiagen, Inc., Valencia, CA), respectively, following the directions of the manufacturer. SIV/17E-Fr proviral and RNA viral loads were quantitated by use of envelope specific primers and probes in a real-time PCR and real time RT-PCR assays. Each sample was quantitated in duplicate and the experiment was performed two times; the sensitivity of detection was 5 copy equivalents/μg of total brain DNA or RNA. The primers and probe for SIV/17E-Fr were the following: forward 5′-CAG CAT CAG CAA GAG TAG ACA TG-3′; reverse 5′-CAA GCC TGC GCA ATT ATC C-3′; probe: 5′-/56-FAM/TCA ATG AGA CTA GTT CTT GTA TAG CCC/3BHQ_1/-3′. The real time PCR cycling was as follows: 1× 95.0°C for 15 min; 45× (95.0°C for 15 sec, 55.0°C for 1 min) data collection and real-time analysis enabled at 60.0°C. For real time RT-PCR an additional step at 50.0°C for 30 min was added.

Amplification, cloning and sequencing of V3-V5 regions of *env*

A 905-bp fragment of the *env* region of SIV/17E-Fr was amplified as previously described (Rivera-Amill, Noel, Jr., Orsini, Tirado, Garcia, Buch, & Kumar, 2007) The fragment was confirmed by agarose electrophoresis prior to cloning into pCR2.1 using the TOPO TA cloning kit (Invitrogen, Carlsbad, CA). Positive clones were identified by colony screening with restriction enzyme digest (EcoRI, Promega) and agarose electrophoresis. Plasmid preparation was performed using the standard protocol of Qiagen Qiaprep Spin Mini Kit. primer set as described above. Clones were sequenced using the M13 forward site on pCR2.1 by the DNA Sequencing Facility of Molecular Cloning Laboratories, South San Francisco, USA.

Sequence analysis and statistics

All sequence files were first manually verified and edited as necessary using the software ChromasLite 2.0 (Technelysium Pty Ltd, Australia). Edited sequences were aligned using BioEdit version 7.0.5.2 (Hall TA,) and Clustal W (Thompson, Higgins et al., 1994). The Clustal W program (runs within BioEdit) was set to perform multiple sequence alignments using the default penalties. Aligned sequences were used to calculate viral nucleotide diversity using the method of Kimura-2 parameter in the program MEGA 3.1(Kumar, Tamura et al., 2004). This

same method was used to quantify nucleotide divergence from the source. Phylogenetic trees were constructed using the program MEGA version 3.1. All phylogenetic analyses used the SIV/17E-Fr inoculum sequence as a reference. The cumulative number of sunonymous and non-synonymous substitutions was estimated using Synonymous/Nonsynonymous Analysis (SNAP; http://hiv-web.lanl.gov), which calculates rates of nucleotide substitution from a set of codon aligned nucleotide sequences, based of the method of Nei and Gojobori (Nei & Gojobori, 1986). Statistical comparisons were done using a two-tailed *t*-test. The statistical cut-off for significance in these analyses was $p=0.05$.

Nucleotide Sequences

Sequences in this report are available from GenBank with accession numbers from GQ290222 to GQ290297.

Acknowledgments

This work was supported by National Institute on Drug Abuse (DA015013, DA025011) and NIGMS-RCMI (RR003050). We also acknowledge the support of the RCMI Molecular Biology Core.

References

1. CDC issues HIV prevention fact sheets for injection drug use. AIDS Policy Law 2002;17:4.
2. HIV diagnoses among injection-drug users in states with HIV surveillance--25 states, 1994-2000. MMWR Morb Mortal Wkly Rep 2003;52:634–636. [PubMed: 12855944]
3. Alcabes P, Friedland G. Injection drug use and human immunodeficiency virus infection. Clin Infect Dis 1995;20:1467–1479. [PubMed: 7548494]
4. Amara RR, Villinger F, Altman JD, Lydy SL, O'Neil SP, Staprans SI, Montefiori DC, Xu Y, Herndon JG, Wyatt LS, Candido MA, Kozyr NL, Earl PL, Smith JM, Ma HL, Grimm BD, Hulsey ML, Miller J, McClure HM, McNicholl JM, Moss B, Robinson HL. Control of a mucosal challenge and prevention of AIDS by a multiprotein DNA/MVA vaccine. Science 2001;292:69–74. [PubMed: 11393868]
5. Centers for Disease Control and Prevention. HIV/AIDS Surveillance Report, 2006. Vol. 18. U.S. Department of Health and Human Services, Centers for Disease Control and Prevention; 2008.
6. Chen MF, Westmoreland S, Ryzhova EV, Martin-Garcia J, Soldan SS, Lackner A, Gonzalez-Scarano F. Simian immunodeficiency virus envelope compartmentalizes in brain regions independent of neuropathology. J Neurovirol 2006;12:73–89. [PubMed: 16798669]
7. Chu TX, Levy JA. Injection drug use and HIV/AIDS transmission in China. Cell Res 2005;15:865–869. [PubMed: 16354561]
8. Chuang LF, Killam KF Jr, Chuang RY. Increased replication of simian immunodeficiency virus in CEM ×174 cells by morphine sulfate. Biochem Biophys Res Commun 1993;195:1165–1173. [PubMed: 8216245]
9. Clements JE, Babas T, Mankowski JL, Suryanarayana K, Piatak M Jr, Tarwater PM, Lifson JD, Zink MC. The central nervous system as a reservoir for simian immunodeficiency virus (SIV): steady-state levels of SIV DNA in brain from acute through asymptomatic infection. J Infect Dis 2002;186:905–913. [PubMed: 12232830]
10. Cohn JA. HIV-1 infection in injection drug users. Infect Dis Clin North Am 2002;16:745–770. [PubMed: 12371125]
11. Dehghani H, Puffer BA, Doms RW, Hirsch VM. Unique pattern of convergent envelope evolution in simian immunodeficiency virus-infected rapid progressor macaques: association with CD4-independent usage of CCR5. J Virol 2003;77:6405–6418. [PubMed: 12743298]
12. Des J. Psychoactive drug use and progression of HIV infection. J Acquir Immune Defic Syndr Hum Retrovirol 1999;20:272–274. [PubMed: 10077176]
13. Dunfee R, Thomas ER, Gorry PR, Wang J, Ancuta P, Gabuzda D. Mechanisms of HIV-1 neurotropism. Curr HIV Res 2006;4:267–278. [PubMed: 16842080]

14. Flaherty MT, Hauer DA, Mankowski JL, Zink MC, Clements JE. Molecular and biological characterization of a neurovirulent molecular clone of simian immunodeficiency virus. J Virol 1997;71:5790–5798. [PubMed: 9223467]
15. Guo CJ, Li Y, Tian S, Wang X, Douglas SD, Ho WZ. Morphine enhances HIV infection of human blood mononuclear phagocytes through modulation of beta-chemokines and CCR5 receptor. J Investig Med 2002;50:435–442.
16. Hall TA. BioEdit: A user friendly biological sequence alignment editor and analysis program for windows 95/98/NT. Nucl Acids Symp Ser 41:95–98. Ref Type: Generic.
17. Hicks A, Potula R, Sui YJ, Villinger F, Pinson D, Adany I, Li Z, Long C, Cheney P, Marcario J, Novembre F, Mueller N, Kumar A, Major E, Narayan O, Buch S. Neuropathogenesis of lentiviral infection in macaques: roles of CXCR4 and CCR5 viruses and interleukin-4 in enhancing monocyte chemoattractant protein-1 production in macrophages. Am J Pathol 2002;161:813–822. [PubMed: 12213709]
18. Kinsey NE, Anderson MG, Unangst TJ, Joag SV, Narayan O, Zink MC, Clements JE. Antigenic variation of SIV: mutations in V4 alter the neutralization profile. Virology 1996;221:14–21. [PubMed: 8661410]
19. Kumar R, Orsoni S, Norman L, Verma AS, Tirado G, Giavedoni LD, Staprans S, Miller GM, Buch SJ, Kumar A. Chronic morphine exposure causes pronounced virus replication in cerebral compartment and accelerated onset of AIDS in SIV/SHIV-infected Indian rhesus macaques. Virology 2006;354:192–206. [PubMed: 16876224]
20. Kumar R, Torres C, Yamamura Y, Rodriguez I, Martinez M, Staprans S, Donahoe RM, Kraiselburd E, Stephens EB, Kumar A. Modulation by morphine of viral set point in rhesus macaques infected with simian immunodeficiency virus and simian-human immunodeficiency virus. J Virol 2004;78:11425–11428. [PubMed: 15452267]
21. Kumar S, Tamura K, Nei M. MEGA3: Integrated software for Molecular Evolutionary Genetics Analysis and sequence alignment. Brief Bioinform 2004;5:150–163. [PubMed: 15260895]
22. Kuwata T, Dehghani H, Brown CR, Plishka R, Buckler-White A, Igarashi T, Mattapallil J, Roederer M, Hirsch VM. Infectious molecular clones from a simian immunodeficiency virus-infected rapid-progressor (RP) macaque: evidence of differential selection of RP-specific envelope mutations in vitro and in vivo. J Virol 2006;80:1463–1475. [PubMed: 16415023]
23. Nei M, Gojobori T. Simple methods for estimating the numbers of synonymous and nonsynonymous nucleotide substitutions. Mol Biol Evol 1986;3:418–426. [PubMed: 3444411]
24. Noel RJ Jr, Kumar A. Virus replication and disease progression inversely correlate with SIV tat evolution in morphine-dependent and SIV/SHIV-infected Indian rhesus macaques. Virology 2006;346:127–138. [PubMed: 16313937]
25. Noel RJ Jr, Kumar A. SIV Vpr evolution is inversely related to disease progression in a morphine-dependent rhesus macaque model of AIDS. Virology 2007;359:397–404. [PubMed: 17064752]
26. Noel RJ Jr, Marrero-Otero Z, Kumar R, Chompre-Gonzalez GS, Verma AS, Kumar A. Correlation between SIV Tat evolution and AIDS progression in cerebrospinal fluid of morphine-dependent and control macaques infected with SIV and SHIV. Virology 2006;349:440–452. [PubMed: 16643974]
27. Nyland SB, Specter S, Im-Sin J, Ugen KE. Opiate effects on in vitro human retroviral infection. Adv Exp Med Biol 1998;437:91–100. [PubMed: 9666261]
28. Otto C, Puffer BA, Pohlmann S, Doms RW, Kirchhoff F. Mutations in the C3 region of human and simian immunodeficiency virus envelope have differential effects on viral infectivity, replication, and CD4-dependency. Virology 2003;315:292–302. [PubMed: 14585332]
29. Reimann KA, Li JT, Veazey R, Halloran M, Park IW, Karlsson GB, Sodroski J, Letvin NL. A chimeric simian/human immunodeficiency virus expressing a primary patient human immunodeficiency virus type 1 isolate env causes an AIDS-like disease after in vivo passage in rhesus monkeys. J Virol 1996a; 70:6922–6928. [PubMed: 8794335]
30. Reimann KA, Li JT, Voss G, Lekutis C, Tenner-Racz K, Racz P, Lin W, Montefiori DC, Lee-Parritz DE, Lu Y, Collman RG, Sodroski J, Letvin NL. An env gene derived from a primary human immunodeficiency virus type 1 isolate confers high in vivo replicative capacity to a chimeric simian/human immunodeficiency virus in rhesus monkeys. J Virol 1996b;70:3198–3206. [PubMed: 8627800]

31. Rivera-Amill V, Noel RJ Jr, Orsini S, Tirado G, Garcia JM, Buch S, Kumar A. Variable region 4 of SIV envelope correlates with rapid disease progression in morphine-exposed macaques infected with SIV/SHIV. Virology 2007;358:373–383. [PubMed: 17011009]

32. Ryzhova E, Whitbeck JC, Canziani G, Westmoreland SV, Cohen GH, Eisenberg RJ, Lackner A, Gonzalez-Scarano F. Rapid progression to simian AIDS can be accompanied by selection of CD4-independent gp120 variants with impaired ability to bind CD4. J Virol 2002;76:7903–7909. [PubMed: 12097605]

33. Singh DK, McCormick C, Pacyniak E, Griffin D, Pinson DM, Sun F, Berman NE, Stephens EB. Pathogenic and nef-interrupted simian-human immunodeficiency viruses traffic to the macaque CNS and cause astrocytosis early after inoculation. Virology 2002;296:39–51. [PubMed: 12036316]

34. Suzuki S, Chuang AJ, Chuang LF, Doi RH, Chuang RY. Morphine promotes simian acquired immunodeficiency syndrome virus replication in monkey peripheral mononuclear cells: induction of CC chemokine receptor 5 expression for virus entry. J Infect Dis 2002;185:1826–1829. [PubMed: 12085334]

35. Thompson JD, Higgins DG, Gibson TJ. CLUSTAL W: improving the sensitivity of progressive multiple sequence alignment through sequence weighting, position-specific gap penalties and weight matrix choice. Nucleic Acids Res 1994;22:4673–4680. [PubMed: 7984417]

36. Tirado G, Kumar A. Evolution of SIV envelope in morphine-dependent rhesus macaques with rapid disease progression. AIDS Res Hum Retroviruses 2006;22:114–119. [PubMed: 16438654]

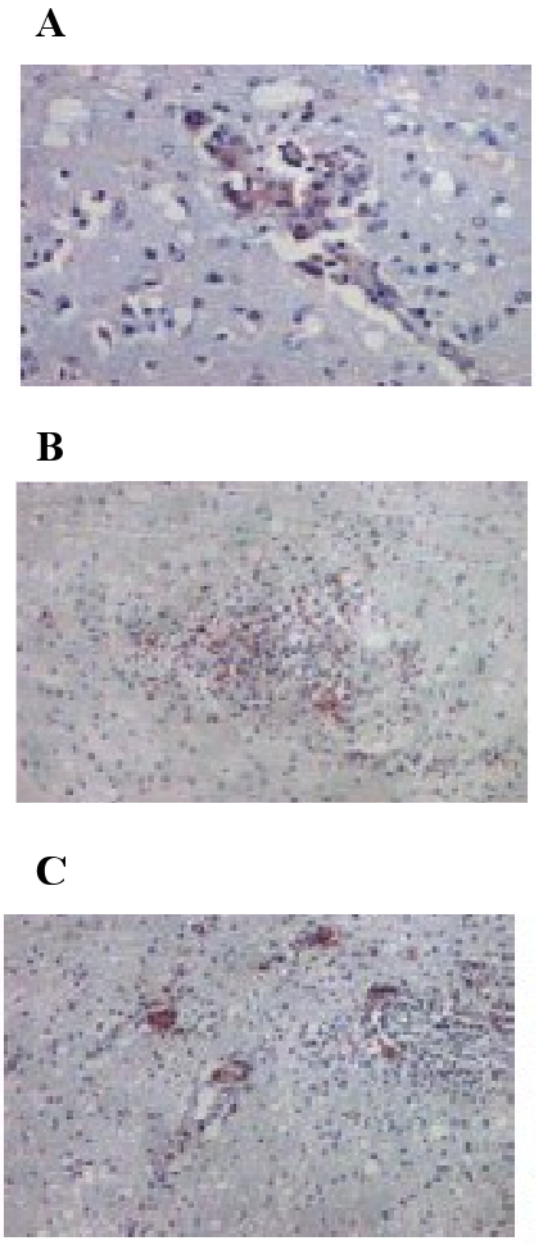

Figure 1.
Pathological changes in morphine-dependent rapid progressor with neurological symptoms. Immunohistochemical analyses were performed on paraffin-embedded tissues from macaque 1/28Q as described in the Materials and Methods. Panels: A, accumulation of macrophages in the perivascular region; B, focal histiocytic nodules; C, multi-nucleated giant cells.

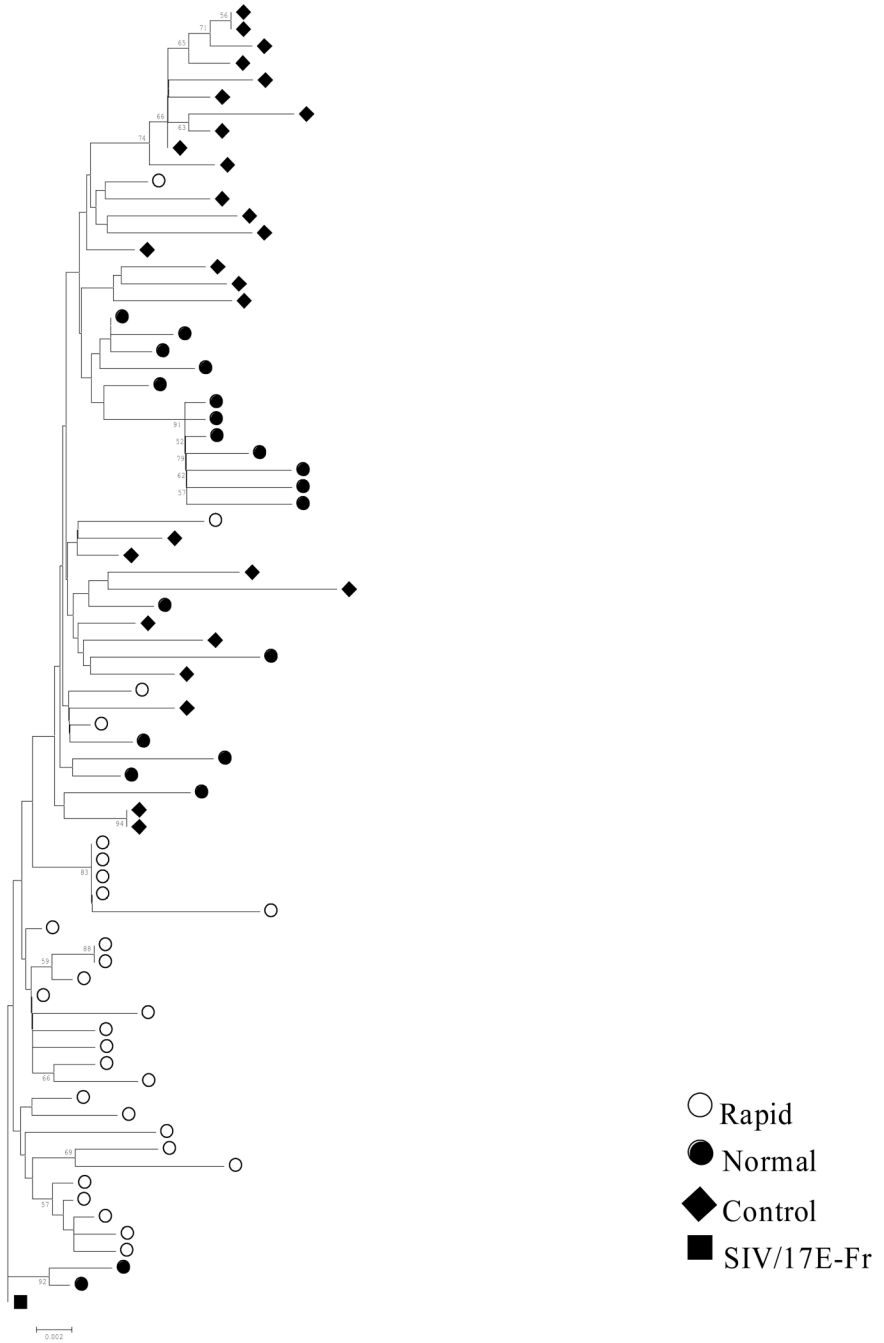

Figure 2.

Boostrap Neighbor-Joining trees of *env* V3-V5 sequences. Envelope sequences were obtained from brain tissue of morphine-dependent rapid progressors (red circles), morphine-dependent normal progressors (green circles) and control macaques (blue diamonds) infected with SIV/17E-Fr, $SHIV_{KU-1B}$ and $SHIV_{89.6}P$. The phylogenetic trees were generated using the MEGA 3.1 program and boostrap values were performed on 500 replicates and those >50 are indicated at the nodes. Nodes where no value is indicated were not supported at this level. The trees were rooted using the corresponding sequence from SIV/17E-Fr (black square).

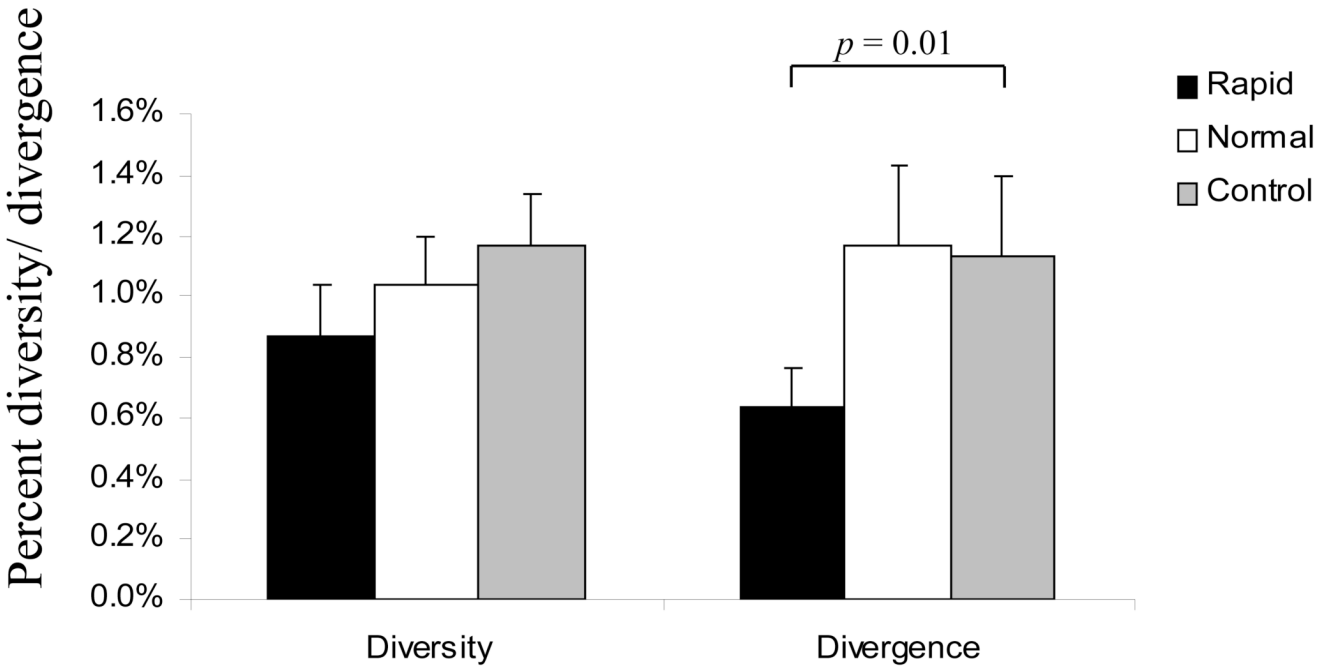

Figure 3.

Viral molecular diversity and divergence of brain-derived *env* V3-V5 sequences obtained from morphine-dependent and control macaques infected with SIV/17E-Fr, $SHIV_{KU-1B}$ and $SHIV_{89.6}P$. The proviral *env* sequences were aligned and used to calculate diversity and divergence using MEGA 3.1. The mean percent diversity and divergence are plotted for each group. Error bars indicate mean of standard error.

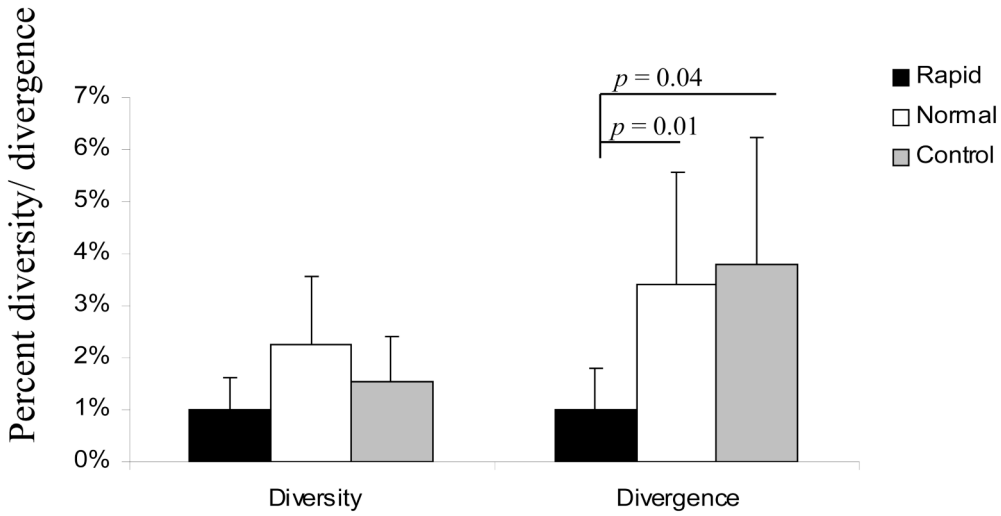

Figure 4.

Viral molecular diversity and divergence of brain-derived *env* V4 sequences obtained from morphine-dependent and control macaques infected with SIV/17E-Fr, $SHIV_{KU-1B}$ and $SHIV_{89.6}P$. The proviral *env* sequences were aligned and used to calculate diversity and divergence using MEGA 3.1. The mean percent diversity and divergence are plotted for each group. Error bars indicate standard error of the mean.

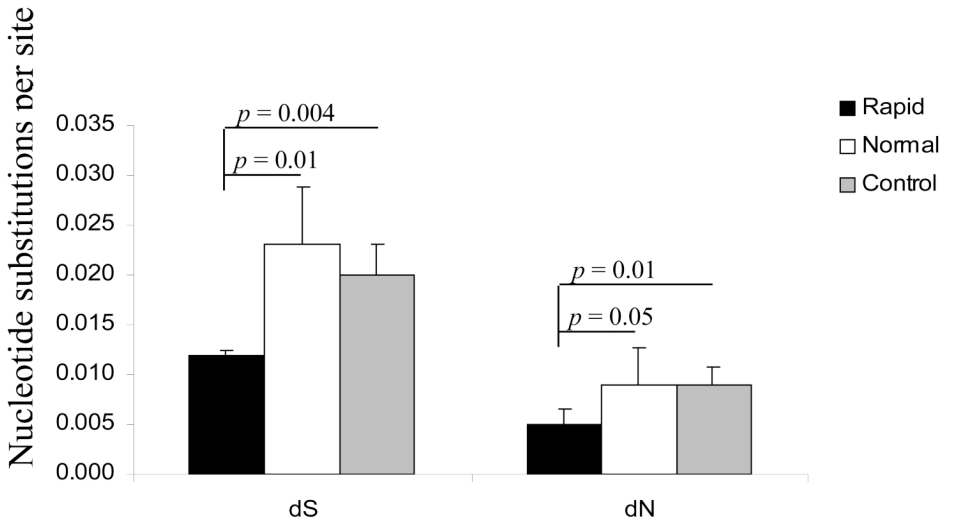

Figure 5.

Rate of substitution at synonymous and non-synonymous sites. SIV *env* V3-V5 nucleotide sequences isolated from brain tissue of morphine-dependent and control macaques were compared to the sequence of the starting molecular clone of SIV/17E-Fr. The numbers of nucleotide changes leading to synonymous (dS) and non-synonymous (dN) mutations were tallied using SNAP, www.hiv.lanl.gov. Error bars indicate standard deviation.

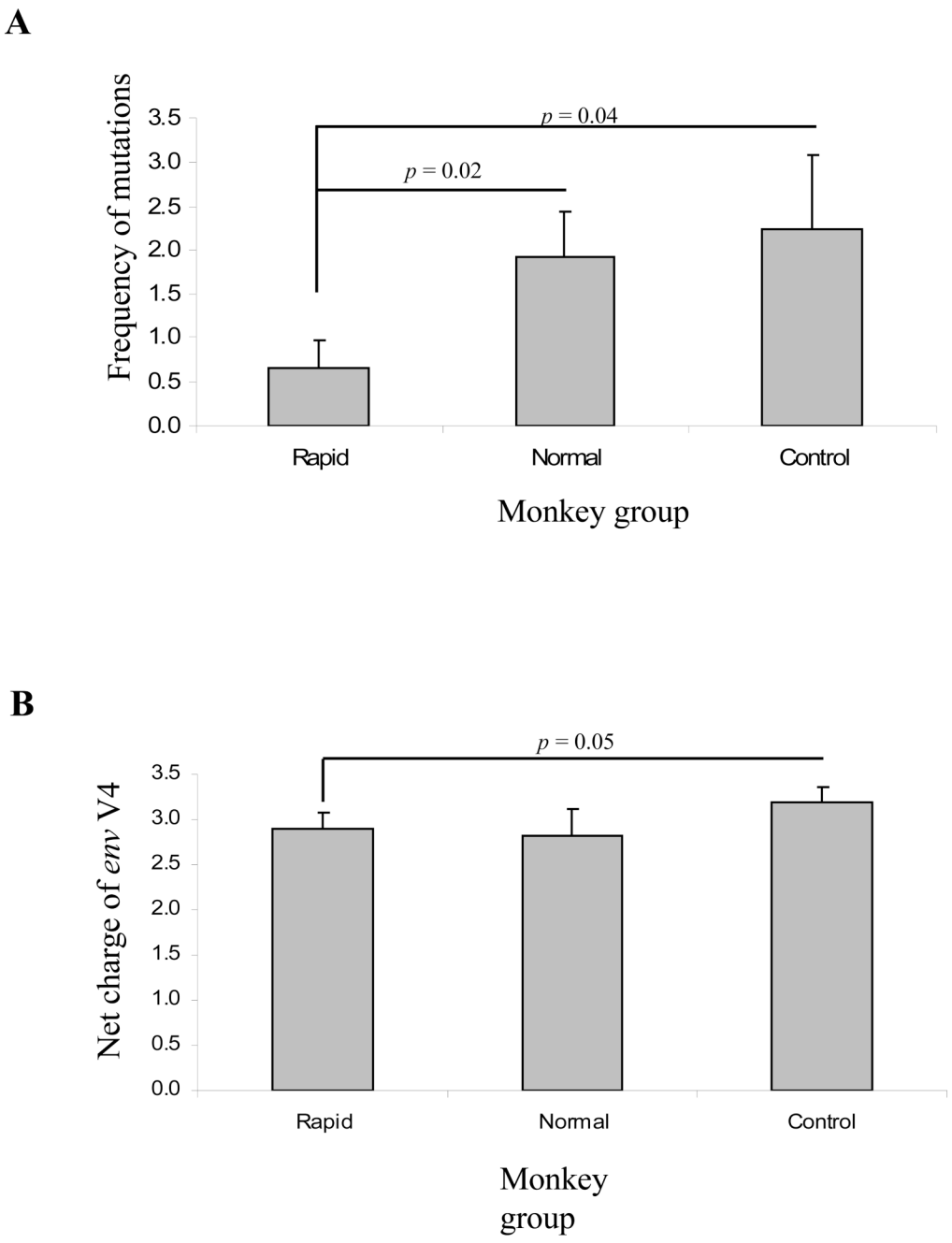

Figure 6.

Mean frequency of amino acid mutations and net charge changes within the V4 loop from brain sequences of morphine-dependent and control macaques infected with SIV/17E-Fr, $SHIV_{KU-1B}$ and $SHIV_{89.6}P$. Panel A, The mean frequency of amino acid mutations was calculated as the total number of mutations in monkey divided by the number of clones. Represented are the averages of mutations per group. Panel B, The net charge of the V4 loop was calculated by subtracting the number of negatively charged amino acids from the number of positively charged amino acids. Represented are the averages of the net charge per group. Error bars indicate standard deviation.

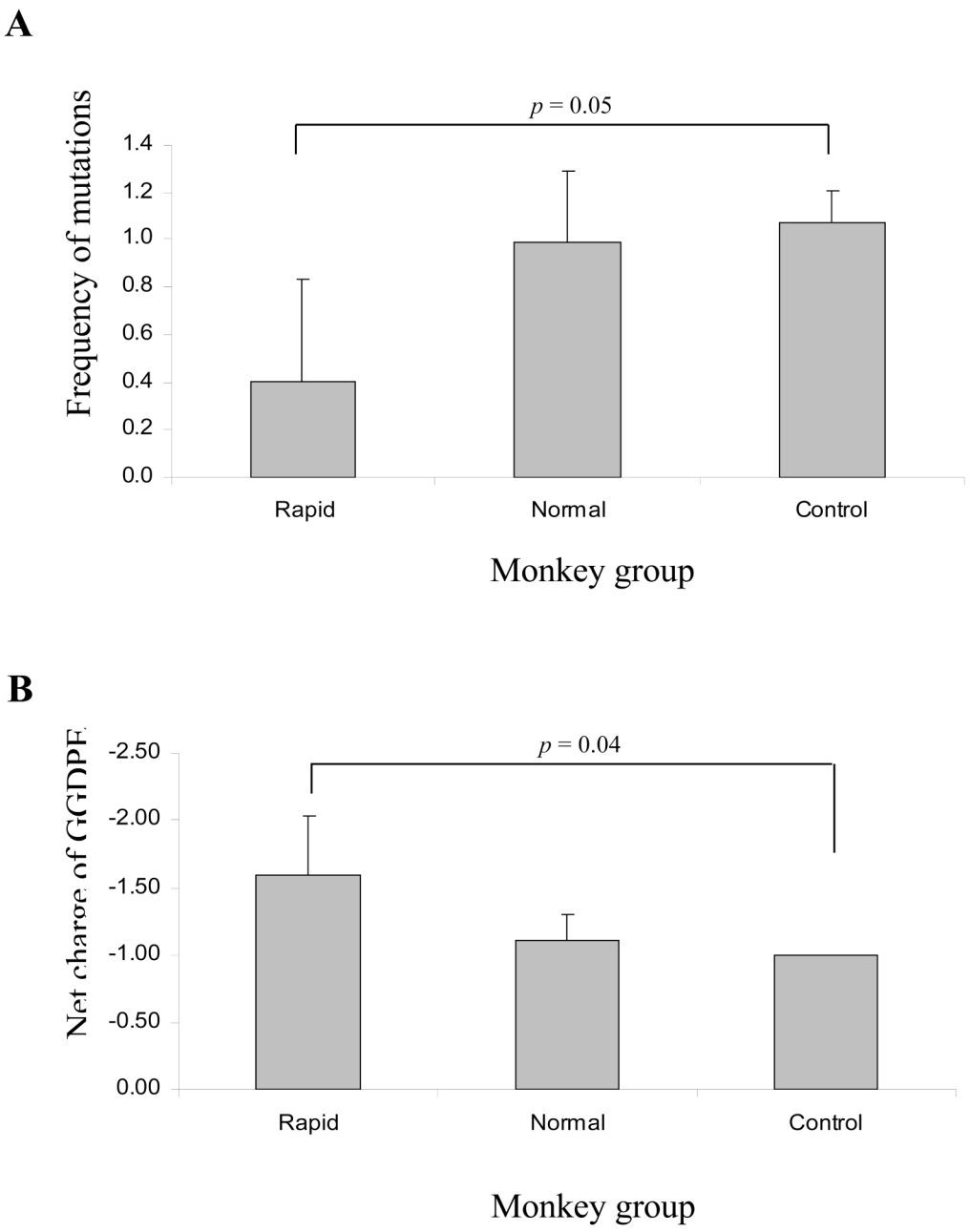

Figure 7.

Mean frequency of amino acid mutations and net charge changes within the GGDPE motif from brain sequences of morphine-dependent and control macaques infected with SIV/17E-Fr, $SHIV_{KU-1B}$ and $SHIV_{89.6}P$. Panel A, The mean frequency of amino acid mutations was calculated as the total number of mutations in monkey divided by the number of clones. Represented are the averages of mutations per group. Panel B, The net charge of the GGDPE motif was calculated by subtracting the number of negatively charged amino acids from the number of positively charged amino acids. Represented are the averages of the net charge per group. Error bars indicate standard deviation.

Table 1

Summary of clinical data.

Macaque	Survival[a] (weeks, pi)	CD4$^+$ T cells[b]	Viral load (×10^4 RNA copies/ml)		Brain proviral load (×10^3 copies/μg of DNA)	Brain RNA viral load (×10^2 copies/μg of RNA)	SAIDS[f]
			Plasma	CSF			
Morphine-							
Rapid							
1/04L	18	2.9	3340	226	0.007	12.3	+
1/42N[c]	19	10	10700	111	0.003	7.38	+
1/28Q[c]	20	6	7660	166	0.001	4.93	+
Normal							
1/56L[c]	51	23	436	382	0.0002	4.13	+
1/02N	161	43	2.87	ND[d]	0.03	ND[e]	-
1/52N	161	160	ND[d]	ND[d]	0.0001	4.75	-
Control							
2/02P	60	42	2.56	1.67	0.00003	5.0	+
2/AC42	64	67	.038	ND[d]	0.0005	4.98	+
2/31P	147	503	.236	ND[d]	0.0001	5.34	-

[a] A monkey surviving <24 weeks after infection was considered a rapid disease progressor.

[b] CD4$^+$ T cells are presented as number/ml of blood at the time of necropsy.

[c] The animal developed neurological disorders

[d] Not detectable. The viral load was <20 RNA copies/ml.

[e] Not done

[f] SAIDS: Simian AIDS